Inorg. Chem. **2005**, *44*, 325–335

Structural and Spectroscopic Characterization of First-Row Transition Metal(II) Substituted Blue Copper Model Complexes with Hydrotris(pyrazolyl)borate

Yuki Matsunaga, Kiyoshi Fujisawa,* Naoko Ibi, Yoshitaro Miyashita, and Ken-ichi Okamoto

Department of Chemistry, University of Tsukuba, Tsukuba 305-8571, Japan

Received February 13, 2004

[CuL(SC_6F_5)] (**1**) (L = hydrotris(3,5-diisopropyl-1-pyrazolyl)borate anion) has been reported as a good model for blue copper proteins [Kitajima, N.; Fujisawa, K.; Tanaka, M.; Moro-oka, Y. *J. Am. Chem. Soc.* **1992**, *114*, 9232–9233]. To obtain more structural and spectroscopic insight, the first-row transition metal(II) substituted complexes of Cu(II) (**1**) to Mn(II) (**2**), Fe(II) (**3**), Co(II) (**4**), Ni(II) (**5**), and Zn(II) (**6**) were synthesized and their crystal structures were determined. These model complexes have a distorted tetrahedral geometry arising from the tripodal ligand L. The *d* value, which is defined by the distance from the N_2S basal plane to the metal(II) ion, and the bond angles such as N–M–N and S–M–N are good indicators of these structural distortions. The obtained complexes were characterized by UV–vis absorption, EPR, NMR, far-IR, and FT-Raman spectroscopies and electrochemical and magnetic properties. In UV–vis absorption spectra, the sulfur-to-metal(II) CT bands and the d–d transition bands are observed for **1** and **3**–**5**. For **1**, the strong sulfur to Cu(II) CT band at 663 nm, which is one of the unique properties of blue copper proteins, is observed. The CT energies of the Fe(II) (**3**), Co(II) (**4**), and Ni(II) (**5**) complexes are shifted to higher energy (308 and 355 nm for **3**, 311 and 340 nm for **4**, 357 and 434 nm for **5**) and are almost the same as the corresponding Co(II)- and Ni(II)-substituted blue copper proteins. In the far-IR spectra, three far-IR absorption bands for **2**–**6** at ca. 400, ca. 350, and ca. 310 cm^{-1} are also observed similar to those for **1**. Other properties are consistent with their distorted tetrahedral geometries.

Introduction

The active sites of blue copper proteins play important roles in electron transfer between proteins, but they do not carry out any catalytic reactions.[1−4] Blue copper proteins have unique spectral properties that include a strong sulfur to Cu(II) CT bands (at ca. 600 nm) (which is the origin of its blue color) in the UV−vis absorption spectrum, a small hyperfine structure constant in the EPR spectrum, and a number of bands in the 250−500 cm^{-1} region of the resonance Raman spectrum.[1−4] These properties arise from a distorted tetrahedral geometry in the central Cu(II) ion, which has been revealed by X-ray crystallography.[5] For native blue copper proteins, metal substitutions of the Cu(II) center,[6−15] as well as the mutations of amino acids around the Cu(II) ion,[16] have been studied to understand differences in the interaction between the metal(II) ion and its coordi-

* Author to whom correspondence should be addressed. E-mail: kiyoshif@chem.tsukuba.ac.jp. Tel.: +81-29-853-6922. Fax: +81-29-853-6503.

(1) (a) Solomon, E. I.; Szilagyi, R. K.; DeBeer George, S.; Basumallick, L. *Chem. Rev.* **2004**, *104*, 419. (b) Solomon, E. I.; Randall, D. W.; Glaser, T. *Coord. Chem. Rev.* **2000**, *200*−*202*, 595. (c) Randall, D. W.; Gamelin, D. R.; LaCroix, L. B.; Solomon, E. I. *J. Biol. Inorg. Chem.* **2000**, *5*, 16. (d) Holm, R. H.; Kennepohl, P.; Solomon, E. I. *Chem. Rev.* **1996**, *96*, 2239. (e) Solomon, E. I.; Baldwin, M. J.; Lowery, M. D. *Chem. Rev.* **1992**, *92*, 521.
(2) Messerschmidt, A. *Struct. Bonding (Berlin)* **1998**, *90*, 37.
(3) Adman, E. T. *Adv. Protein Chem.* **1992**, *42*, 145.
(4) Sykes, A. G. *Struct. Bonding (Berlin)* **1990**, *75*, 177.
(5) *Handbook of Metalloproteins*; Messerschmidt, A., Huber, R., Poulos, T., Wieghardt, K., Eds.; John Wiley & Sons: Chichester, U.K., 2001: (a) Freeman, H. C.; Guss, J. M. p 1153. (b) Kolczak, U.; Dennison, C.; Messerschmidt, A.; Canters, G. W. p 1170. (c) Adman, E. T. p 1195. (d) Mathews, F. S. p 1203. (e) Guss, J. M.; Freeman, H. C. p 1215. (f) Nersissian, A. M.; Hart, P. J.; Valentine, J. S. p 1219. (g) Shoham, M. p 1235.
(6) Bonander, N.; Vänngård, T.; Tsai, L.-C.; Langer, V.; Nar, H.; Sjölin, L. *Proteins: Struct., Funct., Genet.* **1997**, *27*, 385.
(7) Moratal, J. M.; Romero, A.; Salgado, J.; Perales-Alarcón, A.; Jiménez, H. R. *Eur. J. Biochem.* **1995**, *228*, 653.
(8) (a) Chen, Z.-W.; Barber, M. J.; McIntire, W. S.; Mathews, F. S. *Acta Crystallogr.* **1998**, *D54*, 253. (b) Nar, H.; Huber, R.; Messerschmidt, A.; Filippou, A. C.; Barth, M.; Jaquinod, M.; van de Kamp, M.; Canters, G. W. *Eur. J. Biochem.* **1992**, *205*, 1123.
(9) Blackwell, K. A.; Anderson, B. F.; Baker, E. N. *Acta Crystallogr.* **1994**, *D50*, 263.

10.1021/ic049814x CCC: $30.25
Published on Web 12/24/2004

nated atoms. These studies provide evidence for why a Cu(II) ion is used as the central metal and how it controls electron-transfer reaction.[17] In this context, much research, including X-ray crystal analysis,[6−9] UV−vis absorption,[10−11] CD and MCD,[12] fluorescence,[13] NMR,[10a,10d,11] EPR,[6,10d] and resonance Raman[11] spectroscopy, has been reported for azurins, which were substituted by transition metal(II) ions such as Co(II) (*Pseudomonas aeruginosa*[6]), Ni(II) (*P. aeruginosa*[7]), Zn(II) (*P. aeruginosa* and *Pseudomonas putida*[8]), and Cd(II) (*Alcaligenes denitrificans*[9]).[18]

The Cu(II) ion in azurin from *P. aeruginosa* has a nearly trigonal arrangement with two imidazole N atoms from His46 and His117 and one thiolate S atom from Cys112 (Chart 1, left).[19] A sulfide S atom from Met121 is found along the trigonal axis at a long distance, reflecting a weak interaction, and a peptide carbonyl O atom (Gly45) is located on the other side of the trigonal N_2S plane at an even longer

Chart 1. Copper coordination Geometry: Azurin[19] (Left), Plastocyanin[20] (Right)

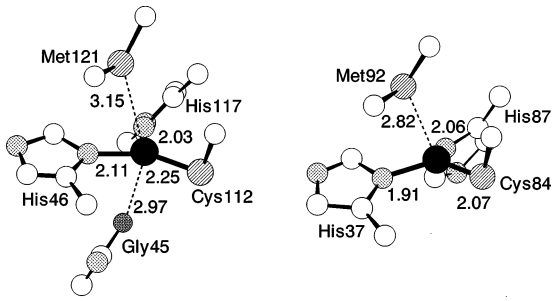

distance. Thus, the structure of Cu(II) ion in azurin takes on a $Cu^{II}N_2S_2$ type distorted tetrahedral geometry. The Cu(II) ion in plastocyanin from *Populus nigra* also has a nearly trigonal-based, distorted tetrahedral geometry with two Cu−N bonds (His37 and His87), a short Cu−S bond (Cys84), and a long Cu−S bond (Met92) (Chart 1, right).[20]

To study the origin of the unique properties of blue copper proteins, many model complexes have been reported.[21] However, these model complexes do not completely reproduce the properties of the protein due to the fact that the Cu(II) ion prefers an octahedral-based conformation, which is stabilized by the Jahn−Teller effect over a tetrahedral conformation. Furthermore, Cu(II)−S bonds dissociate easily and are affected by the reduction of the Cu(II) ion and the formation of a disulfide bond.[1−4,21,22] Much research still focuses on overcoming these synthetic challenges.

The first successful synthesis of a blue copper model complex was [Cu{HB(3,5-Me_2pz)$_3$}($SC_6H_4NO_2$)], made by Ibers and Thompson (HB(3,5-Me_2pz)$_3$ = hydrotris(3,5-dimethyl-1-pyrazolyl)borate anion, $SC_6H_4NO_2$ = 4-nitrobenzenethiolate anion) in 1977.[23] This complex reproduced the intense blue color (λ_{max}, 588 nm (3900 M^{-1} cm^{-1})) and the complicated Cu−S stretching in the resonance Raman spectrum. However, its molecular structure has not been characterized by X-ray analysis. Only the structures of copper(I) thiolato complex K[Cu{HB(3,5-Me_2pz)$_3$}($SC_6H_4NO_2$)][23] and Co(II)-substituted thiolato complex [Co{HB(3,5-Me_2pz)$_3$}(SC_6F_5)][24] were reported. In 1992, we reported structurally characterized copper(II) thiolato complexes [CuL(SC_6F_5)] (**1**) and [CuL($SCPh_3$)] (L = hydrotris(3,5-diisopropyl-1-pyrazolyl)borate anion), in which the Cu(II) ion could have a highly distorted tetrahedral geometry due to the tripodal ligand L which forces a distorted four-coordinate configuration.[25] The distance (*d*) from Cu(II) ion to the N_2S basal plane defined by the three coordinated atoms confirmed this highly distorted tetrahedral configuration. The *d* values of **1** and [CuL($SCPh_3$)] are 0.34 and 0.20 Å,

(10) (a) Salgado, J.; Jiménez, H. R.; Moratal, J. M.; Kroes, S.; Warmerdam, G. C. M.; Canters, G. W. *Biochemistry* **1996**, *35*, 1810. (b) Bilio, A. J. D.; Chang, T. K.; Malmström, B. G.; Gray, H. B.; Karlsson, B. G.; Nordling, M.; Pascher, T.; Lundberg, L. G. *Inorg. Chim. Acta* **1992**, *198*−*200*, 145. (c) Tennent, D. L.; McMillin, D. R. *J. Am. Chem. Soc.* **1979**, *101*, 2307. (d) McMillin, D. R.; Tennent, D. L. *ESR and NMR of Paramagnetic Species in Biological and Related Systems*; Bertini, I., Drago, R. S., Eds.; Reidel: Dordrecht, Holland, 1979; p 369. (e) McMillin. D. R.; Rosenberg, R. C.; Gray, H. B. *Proc. Natl. Acad. Sci. U.S.A.* **1974**, *71*, 4760.

(11) (a) Hannan, J. P.; Davy, S. L.; Moore, G. R.; Eady, R. R.; Andrew, C. R. *J. Biol. Inorg. Chem.* **1998**, *3*, 282. (b) Ferris, N. S.; Woodruff, W. H.; Tennent, D. L.; McMillin, D. R. *Biochem. Biophys. Res. Commun.* **1979**, *88*, 288.

(12) Solomon, E. I.; Rawlings, J.; McMillin, D. R.; Stephens, P. J.; Gray, H. B. *J. Am. Chem. Soc.* **1976**, *98*, 8046.

(13) Hutnik, C. M.; Szabo, A. G. *Biochemistry* **1989**, *28*, 3935.

(14) (a) Donaire, A.; Salgado, J.; Moratal, J.-M. *Biochemistry* **1998**, *37*, 8659. (b) Romero, C.; Moratal, J. M.; Donaire, A. *FEBS Lett.* **1998**, *440*, 93. (c) Vila, A. J.; Ramirez, B. E.; Bilio, A. J. D.; Mizoguchi, T. J.; Richards, J. H.; Gray, H. B. *Inorg. Chem.* **1997**, *36*, 4567. (d) Salgado, J.; Jiménez, H. R.; Donaire, A.; Moratal, J. M. *Eur. J. Biochem.* **1995**, *231*, 358. (e) Moratal, J.-M.; Salgado, J.; Donaire, A.; Jiménez, H. R.; Castells, J. *Inorg. Chem.* **1993**, *32*, 3587. (f) Moratal, J.-M.; Salgado, J.; Donaire, A.; Jiménez, H. R.; Castells, J. *J. Chem. Soc., Chem. Commun.* **1993**, 110. (g) Blaszak, J. A.; Ulrich, E. L.; Markley, J. L.; McMillin, D. R. *Biochemistry* **1982**, *21*, 6253. (h) Hill, H. A. O.; Smith, B. E.; Storm, C. B.; Ambler, R. P. *Biochem. Biophys. Res. Commun.* **1976**, *70*, 783.

(15) Jiménez, H. R.; Salgado, J.; Moratal, J. M.; Morgenstern-Badarau, I. *Inorg. Chem.* **1996**, *35*, 2737.

(16) (a) Farver, O.; Jeuken, L. J. C.; Canters, G. W.; Pecht, I. *Eur. J. Biochem.* **2000**, *267*, 3123. (b) Kroes, S, J.; Hoitink, C. G.; Andrew, C. R.; Ai, J. Y.; Sanders-Loehr, J.; Messerschmidt, A.; Hagen, W. R.; Canters, G. W. *Eur. J. Biochem.* **1996**, *240*, 342. (c) van Pouderoyen, G.; Andrew, C. R.; Loehr, T. M.; Sanders-Loehr, J.; Mazumdar, S.; Hill, H. A. O.; Canters, G. W. *Biochemistry* **1996**, *35*, 1397. (d) den Blaauwen, T.; Canters, G. W. *J. Am. Chem. Soc.* **1993**, *115*, 1121. (e) Romero, A.; Hoitink, C. W. G.; Nar, H.; Huber, R.; Messerschmidt, A.; Canters, G. W. *J. Mol. Biol.* **1993**, *229*, 1007. (f) Nar, H.; Messerschmidt, A.; Huber, R.; van de Kamp, M.; Canters, G. W. *J. Mol. Biol.* **1991**, *218*, 427. (g) den Blaauwen, T.; van de Kamp, M.; Canters, G. W. *J. Am. Chem. Soc.* **1991**, *113*, 5050.

(17) (a) Crane, B. R.; Di Bilio, A. J.; Winkler, J. R.; Gray, H. B. *J. Am. Chem. Soc.* **2001**, *123*, 11623. (b) Gray, H. B.; Malmström, B. G.; Williams, R. J. P. *J. Biol. Inorg. Chem.* **2000**, *5*, 551 and references therein. (c) Williams, R. J. P. *Eur. J. Biochem.* **1995**, *234*, 363. (d) Malmström, B. G. *Eur. J. Biochem.* **1994**, *223*, 711. (e) Vallee, B. L.; Williams R. J. P. *Proc. Natl. Acad. Sci. U.S.A.* **1968**, *59*, 498.

(18) The structures of other metal substituted blue copper proteins have been reported such as copper-containing nitrite reductase (Zn: Murphy, M. E. P.; Turley, S.; Kukimoto, M.; Nishiyama, M.; Horinouchi, S.; Sasaki, H.; Tanokura, M.; Adman, E. T. *Biochemistry* **1995**, *34*, 12107).

(19) Nar, H.; Messerschmidt, A.; Huber, R.; van de Kamp, M.; Canters, G. W. *J. Mol. Biol.* **1991**, *221*, 765.

(20) Guss, J. M.; Bartunik, H. D.; Freeman, H. C. *Acta Crystallogr.* **1992**, *B48*, 790.

(21) Kitajima, N. *Adv. Inorg. Chem.* **1992**, *39*, 1.

(22) Hellinga, H. W. *J. Am. Chem. Soc.* **1998**, *120*, 10055.

(23) (a) Thompson J. S.; Marks T. J.; Ibers J. A. *J. Am. Chem. Soc.* **1979**, *101*, 4180. (b) Thompson J. S.; Marks T. J.; Ibers. J. A. *Proc. Natl. Acad. Sci. U.S.A.* **1977**, *74*, 3114.

(24) Thompson J. S.; Sorrell T.; Marks T. J.; Ibers J. A. *J. Am. Chem. Soc.* **1979**, *101*, 4193.

(25) Kitajima, N.; Fujisawa, K.; Tanaka, M.; Moro-oka, Y. *J. Am. Chem. Soc.* **1992**, *114*, 9232.

respectively. These values are very similar with those found for azurins (*P. aeruginosa*, 0.10 Å,[5b,19] and *A. denitrificans*, 0.13 Å[5b,26]) and plastocyanins (*P. nigra*, 0.36 Å,[5a,19,25] and *Enteromorpha prolifera*, 0.37 Å[5a,24,27]). In addition, **1** and [CuL(SCPh$_3$)] show an intense blue color around 600 nm (672 nm (5960 M^{-1} cm^{-1}) and 625 nm (6600 M^{-1} cm^{-1})),[25] a unique axial EPR signal (55 and 74 G),[25] and a Cu−S stretching frequency around 400 cm^{-1} (409 and 422 cm^{-1}) by 647 nm laser excitation,[28−29] respectively. Thus, **1** and [CuL(SCPh$_3$)] reproduce the well-known properties of blue copper proteins and serve as good structural model complexes of the active site.[30,31] Moreover, the properties of **1** in coordinating solvents such as DMF dramatically change because the solvent molecule is coordinated to Cu(II) center (EPR parameters: $g_{\|}$ 2.33, $A_{\|}$ 153 G, $g_{\perp}$ 2.07 at 113 K).[21,32,33] Therefore, the EPR spectrum of [Cu{HB(3,5-Me$_2$pz)$_3$}(SC$_6$H$_4$NO$_2$)] was typical for a tetragonal complex, coordinating THF at 77 K.[23]

Very recently, we determined the self-exchange rate constants (3.14×10^5 M^{-1} s^{-1} at 25 °C) for the redox pair of [Cu^{II}L(SC$_6$F$_5$)] and K[Cu^{I}L(SC$_6$F$_5$)] by NMR line-broadening techniques.[34] This value is characteristic of the most labile Cu(II/I) redox systems, including blue copper proteins.[35] Therefore, **1** is not only a good structural model but also a good functional model for blue copper proteins.

Herein, we report the synthesis of metal(II)-substituted complexes of **1** by using the first-row transition metals of Mn(II) (**2**), Fe(II) (**3**), Co(II) (**4**), Ni(II) (**5**), and Zn(II) (**6**) to obtain more insight into the structural and spectroscopic properties of blue copper proteins. This research is also aimed at understanding the relative rigidity of the hydrotris(pyrazolyl)borate ligand L and its ability to accommodate first row transition metal(II) ions. For this reason, a series of metal(II) complexes (**1**−**6**) *with the same ligand* has been synthesized and studied. We have observed subtle angular and torsional variations with the ligand framework to accommodate the ionic radius of the first-transition metal(II) ions and their general coordination structure preference.[36] On the basis of the crystal structures and UV−vis absorption, NMR, EPR, far-IR, and FT-Raman spectral data and electrochemical and magnetic properties, the influences of different central metal(II) ions are discussed. Furthermore, the structures and properties of the Co(II) (**4**) and Ni(II) (**5**) complexes are compared with those of the corresponding metal(II)-substituted azurins.

Experimental Section

Instrumentation. IR and far-IR spectra were recorded on KBr pellets in the 4600−400 cm^{-1} region and on CsI pellets in the 650−100 cm^{-1} region using a JASCO FT/IR-550 spectrophotometer. FT-Raman spectra were recorded on KBr pellets in the 600−200 cm^{-1} region using a Perkin-Elmer Spectrum GX spectrophotometer. UV−vis spectra of **1** (CH_2Cl_2 solution in 260−1400 nm) or **2**−**6** (cyclohexane solution in 200−1700 nm) were measured with a JASCO V-570 spectrophotometer at room temperature using a quartz cell (0.10 cm path length). Low-temperature absorption spectra of **1**−**6** were recorded in CH_2Cl_2 solution at −45 °C on an Otsuka Electronics MCPD-2000 system with an optical fiber attachment (300−1100 nm). The magnetic susceptibilities were measured with a Sherwood MSB-AUTO susceptibility balance apparatus at 296 K for **4**, 293 K for **5**, and 296 K for **6**. Diamagnetic corrections employed tabulated constants.[37] EPR spectra were recorded on a Bruker EMX-T EPR spectrometer as a frozen solution (CH_2Cl_2/$ClCH_2CH_2Cl$ (1:1)) at low temperature in quartz tubes (diameter 5 mm) with an Oxford Instruments liquid-helium cryostat EPR-10 or liquid-nitrogen temperature controller BVT 3000. ^{1}H NMR (600 MHz) and ^{13}C NMR (150 MHz) spectra of **6** were recorded on a Bruker AVANCE−600 at ambient temperature in CD_2Cl_2. ^{1}H NMR (270 MHz) spectra of **3**−**5** were recorded on a JEOL-EX-270 at ambient temperature in CD_2Cl_2. Chemical shifts were reported as δ values downfield from an internal standard $(CH_3)_4Si$. Electrochemical measurements were carried out under argon at 0 °C in solutions of acetone with $(Bu_4N)(ClO_4)$ as a supporting electrolyte using a BAS CV-50W voltammetric analyzer. Nonaqueous Ag/AgCl electrode (BAS, RE-5) and platinum wire were used as reference and auxiliary electrodes, respectively. A platinum disk was used for the working electrode. The ferrocenium/ferrocene couple was measured under the same conditions to correct for the junction potentials both as an internal reference and as a separate solution. The potential values were corrected by assigning the ferrocenium/ferrocene couple a value of 0.50 V versus SCE.[38] Elemental analysis (C, H, N) was performed by the Chemical Analysis Center of the University of Tsukuba.

General Materials. Preparation and handling of all complexes were performed under an argon atmosphere by employing standard Schlenk line techniques. Dichloromethane was distilled from P_2O_5 prior to use. Diethyl ether, tetrahydrofuran, and heptane were carefully purified by refluxing/distilling under an argon atmosphere over sodium benzophenone ketyl.[39] Ethanol, methanol, cyclohexane, and acetone were spectroscopic grade and were used after bubbling with argon gas. $NaSC_6F_5$ and KSC_6F_5 were prepared by the reaction of HSC_6F_5 with 0.8 equiv of NaH in THF and with 0.8 equiv of KOH in ethanol, respectively.

Preparation of Complexes. [CuL(SC$_6$F$_5$)] (1). This complex was prepared by the same procedure as described in the literature.[25]

(26) Baker, E. N. *J. Mol. Biol.* **1988**, *203*, 1071.
(27) Collyer, C. A.; Guss, J. M.; Sugimura, Y.; Yoshizaki, F.; Freeman, H. C. *J. Mol. Biol.* **1990**, *211*, 617.
(28) Qiu, D.; Kilpatrick, L.; Kitajima, N.; Spiro, T. G. *J. Am. Chem. Soc.* **1994**, *116*, 2585.
(29) Randall, D. W.; DeBeer George, S.; Hedman, B.; Hodgson, K. O.; Fujisawa, K.; Solomon, E. I. *J. Am. Chem. Soc.* **2000**, *122*, 11620.
(30) The structural characterizations of **1** and [CuL(SCPh$_3$)] have been published as a communication in ref 25. The M−S stretching analyses of **1**, [CuL(SCPh$_3$)], and [CuL(SCMe$_3$)] have been published by Spiro in ref 28. The detailed electronic structural characterization of only [CuL(SCPh$_3$)] has been performed by Solomon in ref 29.
(31) Holland and Tolman have reported two structural models for blue copper proteins with a highly hindered β-diketiminate. The complexes reproduced the N_2S plane separated from Cu(II) center having N_2S and N_2SS' ligand donor sets. (a) Holland, P. L.; Tolman, W. B. *J. Am. Chem. Soc.* **1999**, *121*, 7270. (b) Holland, P. L.; Tolman, W. B. *J. Am. Chem. Soc.* **2000**, *122*, 6331.
(32) Fujisawa, K. Unpublished results.
(33) Kitajima, N.; Fujisawa, K.; Moro-oka, Y. *J. Am. Chem. Soc.* **1990**, *112*, 3210.
(34) Fujisawa, K.; Fujita, K.; Takahashi, T.; Kitajima, N.; Moro-oka, Y.; Matsunaga, Y.; Miyashita, Y.; Okamoto, K. *Inorg. Chem. Commun.* **2004**, *7*, 1188.
(35) Rorabacher, D. B. *Chem. Rev.* **2004**, *104*, 651 and references therein.
(36) It is a strong point for model complexes. Some transition metal(II) substituted blue copper proteins have been only reported.[6−9]
(37) O'Connor, C. J. *Prog. Irog. Chem.* **1982**, *29*, 203.
(38) Connelly, N. G.; Geiger, W. E. *Chem. Rev.* **1996**, *96*, 877.
(39) Armarego, W. L. F.; Perrin, D. D. *Purification of Laboratory Chemicals*, 4th ed.; Butterworth-Heinemann: Oxford, U.K., 1997.

Table 1. Summary of Crystallographic Data for [ML(SC_6F_5)] (M = Mn (**2**), Fe (**3**), Co (**4**), Ni (**5**), and Zn (**6**))

	2·CH_2Cl_2	**3**·C_7H_{16}	**4**·0.5C_7H_{16}·0.25CH_2Cl_2	**5**·0.5C_7H_{16}·0.25CH_2Cl_2	**6**
formula	$C_{34}H_{48}N_6SF_5BCl_2Mn$	$C_{40}H_{62}N_6SF_5BFe$	$C_{36.75}H_{54.5}N_6SF_5BCl_{0.5}Co$	$C_{36.75}H_{54.5}N_6SF_5BCl_{0.5}Ni$	$C_{33}H_{46}N_6SF_5BZn$
fw	804.50	820.68	794.90	794.66	730.01
cryst system	monoclinic	monoclinic	triclinic	triclinic	monoclinic
space group	$P2_1/c$ (No. 14)	$P2_1/n$ (No. 14)	$P\bar{1}$ (No. 2)	$P\bar{1}$ (No. 2)	$P2_1/n$ (No. 14)
a, Å	9.905(5)	21.843(11)	9.378(3)	9.417(2)	13.983(10)
b, Å	16.032(7)	9.461(4)	16.873(6)	17.684(5)	16.105(11)
c, Å	25.508(12)	21.893(11)	27.892(10)	27.748(8)	18.54(1)
α, deg			80.852(8)	79.623(8)	
β, deg	90.591(6)	99.350(7)	79.621(9)	80.841(9)	114.020(8)
γ, deg			79.401(10)	68.873(7)	
V, Å^3	4050(3)	4465(4)	4231(3)	4217(2)	3814(5)
Z	4	4	4	4	4
D_{calc}, g/cm^3	1.319	1.221	1.248	1.251	1.271
cryst size, mm^3	0.25 × 0.12 × 0.12	0.30 × 0.25 × 0.05	0.50 × 0.50 × 0.10	0.50 × 0.30 × 0.20	0.35 × 0.20 × 0.25
μ(Mo Kα), cm^{-1}	5.64	4.39	5.41	5.96	7.53
F(000)	1676	1744	1674	1678	1528
temp, °C	−61	−61	−89	−89	−61
2θ range, deg	5−55	5−55	5−55	5−55	5−55
reflcns collcd	33 820	36 931	34 161	34 566	30 469
unique reflcns	9246	10 199	19 051	19 108	8435
R_{int}	0.049	0.060	0.050	0.050	0.090
no. of observns	3220 ($I > 3\sigma(I)$)	4487 ($I > 3\sigma(I)$)	14 878 ($I > 3\sigma(I)$)	13 409 ($I > 3\sigma(I)$)	4640 ($I > 3\sigma(I)$)
no. of variables	499	549	1002	1047	470
reflcn/param ratio	6.45	8.17	14.85	12.81	9.87
R^a	0.067	0.063	0.074	0.068	0.077
$R_w{}^a$	0.063	0.057	0.084	0.073	0.081
goodness of fit	1.55	1.79	3.92	2.55	2.65
max/min peak, e/Å^3	0.92/−0.75	0.56/−0.37	1.41/−1.06	1.07/−1.00	0.65/−0.55

[a] $R = \Sigma||F_o| - |F_c||/\Sigma|F_o|$; $R_w = [(\Sigma w(|F_o| - |F_c|)^2/\Sigma wF_o^2)]^{1/2}$, $w = 1/\sigma^2(|F_o|)$.

To the solution of the binuclear hydroxo complex [(CuL)$_2$(μ-OH)$_2$][40] (0.500 g, 0.46 mmol) in dichloromethane/heptane (50 cm^3) (3:2, v/v) was added pentafluorobenzenethiol (0.15 cm^3, 1.12 mmol) with cooling at −20 °C. The solution was stirred for 2.5 h, and then the solvent was removed in vacuo at the same temperature. The resultant blue powder was recrystallized from dichloromethane/heptane at −30 °C, and blue crystals were formed. Single crystals were obtained from dichloromethane/pentane/*n*-octane at −20 °C. Yield: 88% (0.59 g). Anal. Calcd for $C_{33}H_{46}N_6F_5SBCu$: C, 54.43; H, 6.37; N, 11.54. Found: C, 54.74; H, 6.28; N, 11.61. IR ($\tilde{\nu}$/cm^{-1}): 2967 vs, 2545 m, 1537 m, 1508 vs, 1478 vs, 1174 s, 1055 s, 976 s, 858 s, 791 m. Far-IR ($\tilde{\nu}$/cm^{-1}): 522 m, 406 s, 350 m, 311 m, 243 vs, 221 s, 199 s. (Symbols: vs, very strong; s, strong; m, medium; w, weak.) UV−vis absorption [CH_2Cl_2, rt (room temperature), λ_{max}/nm (ϵ/M^{-1} cm^{-1})]: 362 (1170), 414 (shoulder, 620), 663 (5980), 1040 (1170). UV−vis absorption [CH_2Cl_2, −45 °C, λ_{max}/nm (ϵ/M^{-1} cm^{-1})]: 362 (1320), 420 (shoulder, 590), 670 (5960), 1028 (1300). EPR (CH_2Cl_2/$ClCH_2CH_2Cl$, 140 K): $g_{\|}$ 2.32, $A_{\|}$ 52 G, $g_{\perp}$ 2.10. Cyclic voltammetry (acetone vs Fc^+/Fc /mV): −468 (ΔE = 109 mV).

[MnL(SC_6F_5)] (2). To the solution of the binuclear hydroxo complex [(MnL)$_2$(μ-OH)$_2$][41−42] (0.471 g, 0.44 mmol) in dichloromethane (50 cm^3) was added pentafluorobenzenethiol (0.14 cm^3, 1.05 mmol) with cooling at 0 °C. The solution was stirred for 2.5 h, and then the solvent was removed in vacuo. The resultant white powder was recrystallized from dichloromethane at −15 °C, and white crystals were formed. Yield: 32% (0.20 g). Anal. Calcd for $C_{33}H_{46}N_6F_5SBMn$: C, 53.73; H, 6.24; N, 11.31. Found: C, 53.88; H, 6.33; N, 11.33. IR ($\tilde{\nu}$/cm^{-1}): 2966 vs, 2557 m, 1536 m, 1506 vs, 1476 vs, 1168 s, 1053 s, 969 s, 862 s, 793 m. Far-IR ($\tilde{\nu}$/cm^{-1}): 516 m, 399 s, 339 m, 334 m, 308 m, 199 vs. FT-Raman ($\tilde{\nu}$/cm^{-1}): 511 vs, 489, 473, 444 s, 414 w, 385 s, 351 m, 332 m, 308 m, 238 s. UV−vis absorption [cyclohexane, rt, λ_{max}/nm (ϵ/M^{-1} cm^{-1})]: 218 (39 800), 264 (16 200). EPR (CH_2Cl_2/$ClCH_2CH_2Cl$, 20 K): g 3.91.

[FeL(SC_6F_5)] (3). The mononuclear chloro complex [FeCl(L)][43] (0.409 g, 0.73 mmol) and potassium salt of pentafluorobenzenethiol (0.208 g, 0.87 mmol) were dissolved in THF (30 cm^3) with cooling at −15 °C. After being stirred for 2 h, the solution was filtered. The filtrate was concentrated to dryness in vacuo. The resultant slightly brown colored solid was recrystallized from dichloromethane/heptane at −30 °C, and then white crystals were formed. Yield: 49% (0.26 g). Anal. Calcd for $C_{33}H_{46}N_6F_5SBFe$: C, 55.01; H, 6.43; N, 11.66. Found: C, 54.84; H, 6.55; N, 10.90. IR ($\tilde{\nu}$/cm^{-1}): 2966 vs, 2558 m, 1536 m, 1505 vs, 1475 vs, 1169 s, 1051 s, 969 s, 858 s, 794 m. Far-IR ($\tilde{\nu}$/cm^{-1}): 519 s, 399 s, 347 m, 309 m, 216 s, 197 vs. UV−vis absorption [cyclohexane, rt, λ_{max}/nm (ϵ/M^{-1} cm^{-1})]: 210 (28 050), 242 (14 740), 268 (9400), 308 (5940), 355 (1390), 599 (60), 1360 (95). UV−vis absorption [CH_2Cl_2, −45 °C, λ_{max}/nm (ϵ/M^{-1} cm^{-1})]: 309 (4290), 343 (shoulder, 1050). ^{1}H NMR (CD_2Cl_2, 270 MHz, 296 K): δ −11.76 (s, 1H, B*H*), 3.83 (br, 18H, CH*Me*$_2$), 4.07 (br, 18H, CH*Me*$_2$), 10.98 (br, 3H, C*H*Me$_2$), 16.15 (s, 3H, C*H*Me$_2$), 66.11 (s, 3H, *pz*).

[CoL(SC_6F_5)] (4). The synthesis was carried out by the same method as **2** using [(CoL)$_2$(μ-OH)$_2$][42] (0.153 g, 0.14 mmol) and pentafluorobenzenethiol (0.042 cm^3, 0.31 mmol). Blue crystals were obtained by recrystallization from dichloromethane/heptane at −30 °C. Yield: 40% (0.081 g). Anal. Calcd for $C_{33}H_{46}N_6F_5SBCo$: C, 54.78; H, 6.41; N, 11.62. Found: C, 54.87; H, 6.36; N, 11.40. IR ($\tilde{\nu}$/cm^{-1}): 2967 vs, 2551 m, 1536 m, 1506 vs, 1476 vs, 1167 s, 1052 s, 970 s, 860 s, 792 m. Far-IR ($\tilde{\nu}$/cm^{-1}): 519 s, 399 vs, 346

(40) (a) Kitajima, N.; Fujisawa, K.; Fujimoto, C.; Moro-oka, Y.; Hashimoto, S.; Kitagawa, T.; Toriumi, K.; Tatsumi, K.; Nakamura, A. *J. Am. Chem. Soc.* **1992**, *114*, 1277. (b) Kitajima, N.; Fujisawa, K.; Moro-oka, Y. *Inorg. Chem.* **1990**, *29*, 357.
(41) Kitajima, N.; Singh, U. P.; Amagai, H.; Osawa, M.; Moro-oka, Y. *J. Am. Chem. Soc.* **1991**, *113*, 7757.
(42) Kitajima, N.; Hikichi, S.; Tanaka, M.; Moro-oka. Y. *J. Am. Chem. Soc.* **1993**, *115*, 5496.
(43) Ito, M.; Amagai, H.; Fukui, H.; Kitajima, N.; Moro-oka, Y. *Bull. Chem. Soc. Jpn.* **1996**, *69*, 1937.

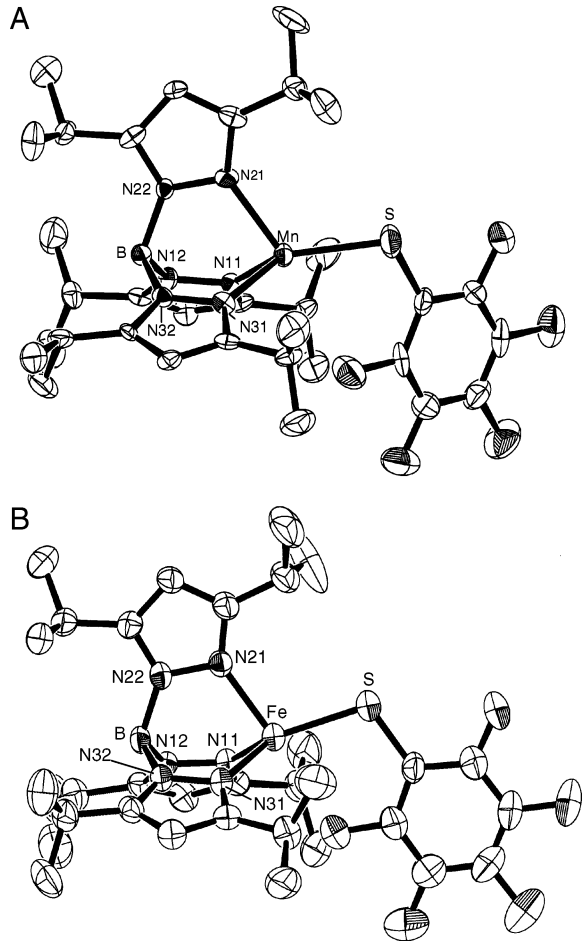

Figure 1. ORTEP representations of (A) [MnL(SC_6F_5)] (**2**) and (B) [FeL(SC_6F_5)] (**3**) (50% probability thermal ellipsoids).

s, 310 m, 224 vs, 211 s. UV−vis absorption [cyclohexane, rt, λ_{max}/nm (ϵ/M^{-1} cm^{-1})]: 215 (22 070), 253 (11 300), 311 (5030), 340 (2930), 430 (650), 605 (broad, 1170), 812 (140), 1479 (115). UV−vis absorption [CH_2Cl_2, −45 °C, λ_{max}/nm (ϵ/M^{-1} cm^{-1})]: 312 (5000), 338 (3149), 420 (shoulder, 452), 599 (1121), 809 (148). Magnetic moment (μ_{eff}/μ_B, 296 K): 4.62. EPR (CH_2Cl_2/$ClCH_2$-CH_2Cl, 20 K): g_1 5.90, g_2 2.66, g_3 1.74. ^{1}H NMR (CD_2Cl_2, 270 MHz, 296 K): δ −13.85 (br, 1H, B*H*), −3.26 (br, 3H, C*H*Me_2), 3.19 (s, 18H, CH*Me*$_2$), 3.84 (s, 18H, CH*Me*$_2$), 8.14 (s, 3H, C*H*Me_2), 73.67 (s, 3H, *pz*).

[NiL(SC_6F_5)] (5). The synthesis was carried out by the same method as **2** using [$(NiL)_2(\mu$-$OH)_2$][42] (0.161 g, 0.15 mmol) and pentafluorobenzenethiol (0.044 cm^3, 0.33 mmol). Orange crystals were obtained by recrystallization from dichloromethane/heptane at −15 °C. Yield: 25% (0.053 g). Anal. Calcd for $C_{33}H_{46}N_6F_5$-SBNi: C, 54.80; H, 6.41; N, 11.62. Found: C, 54.53; H, 6.38; N, 11.41. IR ($\tilde{\nu}$/cm^{-1}): 2966 vs, 2549 m, 1537 m, 1506 vs, 1476 vs, 1176 s, 1054 s, 969 s, 862 s, 795 m. Far-IR ($\tilde{\nu}$/cm^{-1}): 526 s, 399 vs, 349 s, 310 m, 221 vs. UV−vis absorption [cyclohexane, rt, λ_{max}/nm (ϵ/M^{-1} cm^{-1})]: 210 (32 100), 246 (11 310), 357 (1850), 434 (3100), 804 (145), 1400 (35). UV−vis absorption [CH_2Cl_2, −45 °C, λ_{max}/nm (ϵ/M^{-1} cm^{-1})]: 354 (2150), 427 (3360), 798 (broad, 160). Magnetic moment (μ_{eff}/μ_B, 293 K): 3.30. ^{1}H NMR (CD_2Cl_2, 270 MHz, 296 K): δ −11.24 (br, 1H, B*H*), −4.20 (br, 3H, C*H*Me_2), −0.12 (s, 18H, CH*Me*$_2$), 3.21 (s, 18H, CH*Me*$_2$), 4.53 (s, 3H, C*H*Me_2), 81.09 (s, 3H, *pz*).

[ZnL(SC_6F_5)] (6). The synthesis was carried out by the same method as **3** using [ZnBr(L)][42] (0.692 g, 1.13 mmol) and the sodium

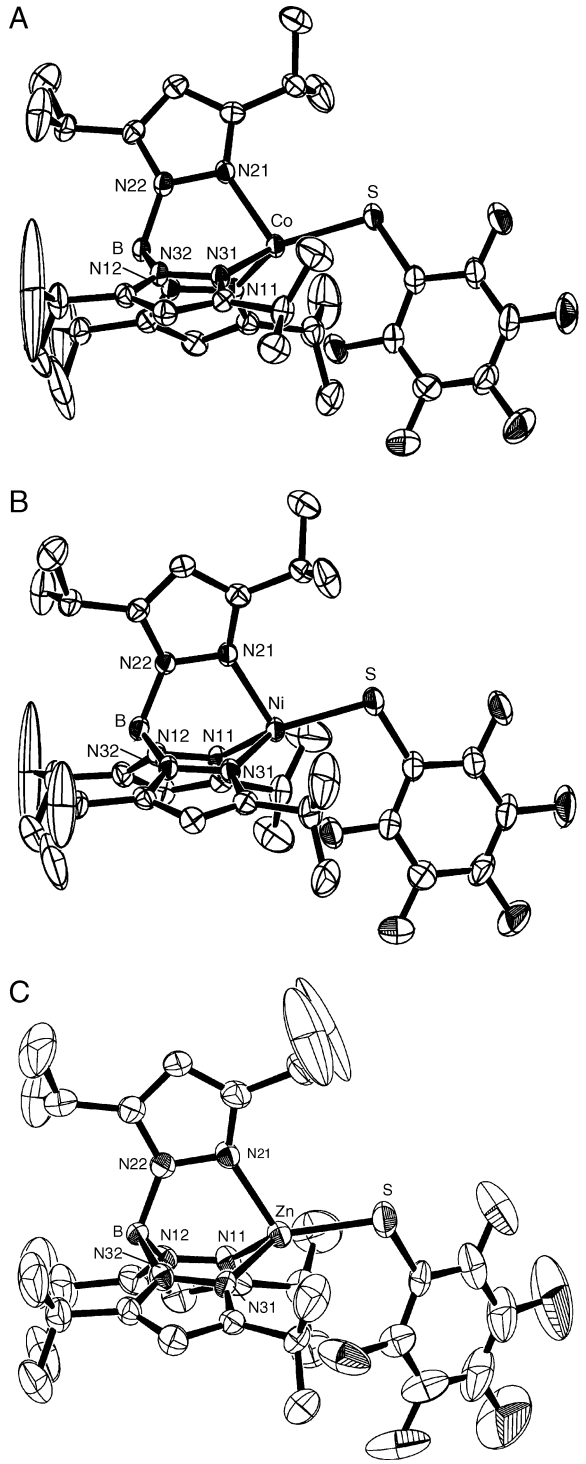

Figure 2. ORTEP representations of (A) [CoL(SC_6F_5)] (**4A**), (B) [NiL(SC_6F_5)] (**5A**), and (C) [ZnL(SC_6F_5)] (**6**) (50% probability thermal ellipsoids).

salt of pentafluorobenzenethiol (0.371 g, 1.67 mmol). White crystals were obtained by recrystallization from dichloromethane/methanol at −15 °C. Single crystals for X-ray analysis were obtained by the slow evaporation of the dichloromethane/heptane solution at room temperature. Yield: 53% (0.44 g). Anal. Calcd for $C_{33}H_{46}N_6F_5$-SBZn: C, 54.29; H, 6.35; N, 11.51. Found: C, 54.20; H, 6.38; N, 11.36. IR ($\tilde{\nu}$/cm^{-1}): 2967 vs, 2557 m, 1538 m, 1508 vs, 1479 vs, 1172 s, 1053 s, 972 s, 862 s, 795 m. Far-IR ($\tilde{\nu}$/cm^{-1}): 520 s, 402 s, 343 s, 310 m, 191 vs. FT-Raman ($\tilde{\nu}$/cm^{-1}): 512 vs, 444 s, 413 w, 401 s, 385 s, 366 w, 339 m, 311 w, 263 s, 219 s, 192 s. UV−

Table 2. Selected Bond Distances (Å) and Angles (deg) for Complexes **1**−**6** and Blue Copper Proteins and Metal-Substituted Ones

	M−S	M−N11	M−N21	M−N31	S−M−N11	S−M−N21	S−M−N31	N11−M−N31	M/N11N31S plane
Cu (**1**)[a]	2.176(4)	2.037(9)	2.119(8)	1.930(9)	122.7(3)	112.7(2)	134.6(3)	90.9(3)	0.34
Mn (**2**)	2.385(3)	2.121(6)	2.125(6)	2.119(6)	128.3(2)	118.3(2)	129.6(2)	90.2(2)	0.43
Fe (**3**)	2.288(2)	2.045(4)	2.073(4)	2.055(4)	131.5(1)	107.2(1)	129.3(1)	94.5(2)	0.26
Co (**4A**)	2.267(1)	2.001(3)	2.026(3)	2.025(3)	129.6(1)	107.82(9)	128.31(9)	94.9(1)	0.32
Co (**4B**)	2.265(1)	2.013(4)	2.039(3)	2.034(3)	129.6(1)	107.8(1)	127.8(1)	95.1(1)	0.33
Ni (**5A**)	2.259(2)	1.995(3)	2.004(3)	1.981(4)	128.9(1)	106.8(1)	132.7(1)	92.8(1)	0.28
Ni (**5B**)	2.259(1)	1.990(4)	2.009(3)	2.004(3)	132.8(1)	106.40(8)	128.4(1)	93.2(1)	0.28
Zn (**6**)	2.248(2)	2.019(6)	2.032(4)	2.024(6)	127.4(2)	114.3(2)	126.4(2)	94.4(2)	0.41
[Co(SC_6F_5){HB(3,5-Me_2pz)$_3$}][b]	2.26(1)	1.97(2)	2.01(2)	1.98(2)	138.3(6)	107.7(6)	121.9(6)	93.3(7)	
azurin (*P. aeruginosa*)[c]	2.25(3)	2.11(5)		2.03(7)	133(2)		123(1)	103(2)	0.10
azurin (*A. denitrificans*)[d]	2.14	2.08		2.00	135		119	105	0.13
Co (*P. aeruginosa*)[e]	2.20	2.32		2.25					0.20[f]
Ni (*P. aeruginosa*)[g]	2.39(7)	2.23(9)		2.22(12)	127(5)		123(5)	108(1)	0.18
Zn (*P. aeruginosa*)[h]	2.30	2.01		2.07	128		121	110	0.15[i]
Zn (*P. putida*)[j]	2.12	1.94		1.94	136		118	103	
Cd (*A. denitrificans*)[k]	2.39(5)	2.25(2)		2.21(1)	132(1)		121(1)	106(2)	0.05(1)
plastocyanin (*P. nigra*)[l]	2.07	1.91		2.06	132		121	97	0.36[a]
plastocyanin (*E. prolifera*)[m]	2.12	1.89		2.17	125		120	104	0.37[a]

[a] Reference 25. [b] Reference 24. [c] Reference 19. [d] Reference 26. [e] Reference 6. [f] Reference 11a. [g] Reference 7. [h] Reference 8b. [i] Reference 5b. [j] Reference 8a. [k] Reference 9. [l] Reference 20. [m] Reference 27.

vis absorption [cyclohexane, rt, λ_{max}/nm (ϵ/M^{-1} cm^{-1})]: 210 (31 790), 214 (32 720), 250 (11 990). Magnetic moment (μ_{eff}/μ_B, 296 K): diamagentic. ^{1}H NMR (CD_2Cl_2, 600 MHz, 296 K): δ 1.13 (d, 18H, CH*Me*$_2$), 1.26 (d, 18H, CH*Me*$_2$), 2.95 (m, 3H, C*H*Me$_2$), 3.46 (m, 3H, C*H*Me$_2$), 5.90 (s, 3H, *pz*). ^{13}C NMR (CD_2Cl_2, 150 MHz, 296 K): δ 23.50 (CH*Me*$_2$), 23.53 (CH*Me*$_2$), 26.54 (*C*HMe$_2$), 27.80 (*C*HMe$_2$), 97.76 (pz-*C*-H), 117−147 (C_6F_5), 157.09 (pz-*C*═N), 160.70 (pz-*C*═N).

X-ray Data Collection and Structural Determination. The single crystals of X-ray quality were obtained by recrystallization from dichloromethane solution at −15 °C for **2**, from dichloromethane/heptane solution at −30 °C for **3** and **4**, and from dichloromethane/heptane solution at −15 °C for **5**. The crystals of **6** were obtained by the slow evaporation of the dichloromethane/heptane mixed solution at room temperature. Crystal data and refinement parameters for **2**−**6** are given in Table 1. The diffraction data for all complexes were measured on a Rigaku/MSC Mercury CCD system with graphite-monochromated Mo Kα (λ = 0.710 69 Å) radiation at low temperature for **2**, **3**, and **6** at −61 °C and for **4** and **5** at −89 °C. All crystals were mounted on the tip of glass fiber by heavy-weight oil. The unit cell parameters of each crystal were determined using CrystalClear[44] from 6 images. The crystals to detector distance were ca. 45 mm. Data were collected using 0.5° intervals in ϕ and ω for 30 s/frame of **2** and **4**, for 60 s/frame of **3**, for 35 s/frame of **5**, and for 20 s/frame of **6** to a maximum 2θ value of 55.0°. A total of 744 oscillation images were collected. The highly redundant data sets were reduced using CrystalClear and corrected for Lorentz and polarization effects.[44] An empirical absorption correction was applied for each complex. Structures were solved by direct methods using the program SIR-92.[45] The position of the metal atoms and their first coordination sphere were located from a direct method *E*-map; other non-hydrogen atoms were found in alternating difference Fourier syntheses[46] and least-squares refinement cycles and during the final cycles were refined anisotropically (CrystalStructure).[47−48] Hydrogen atoms were placed in calculated positions. The chlorine atoms of dichloromethane molecule and the carbon atoms of heptane molecule in **4** were not refined anisotropically because of high disorder. The GOF values of **4** and **5** are not good due to disordered solvents. Crystallographic data and structure refinement parameter including the final discrepancies (R and R_w) are listed in Table 1. Crystallographic data have been deposited at the CCDC, 12 Union Road, Cambridge CB2 1EZ, U.K., and copies can be obtained on request, free of charge, by quoting the publication citation and the deposition nos. 230707−230711.

Results and Discussion

General Aspects. Complexes **1**, **2**, **4**, and **5** were synthesized by using binuclear hydroxometal(II) complexes, [(ML)$_2$(μ-OH)$_2$], as starting materials. Complexes **3** and **6** were synthesized by using mononuclear halogenometal(II) complexes, [FeCl(L)] and [ZnBr(L)], as starting materials because [(FeL)$_2$(μ-OH)$_2$] is unstable toward dioxygen[49] and [Zn(L)(OH)]$_n$ (n = 1 or 2) cannot be obtained in a pure form.[42] Complexes **1**−**3** are unstable toward dioxygen and/or temperature, and therefore were handled under an argon atmosphere and kept at low temperature. All complexes are easily soluble in noncoordinating solvents, such as dichloromethane and heptane.

Crystal Structures. The structures of the neutral [ML(SC_6F_5)] complexes (**2**−**6**) are shown in Figures 1 and 2. Important bond distances, bond angles, and structural parameters are summarized in Table 2 including those of **1**. All of the complexes **1**−**6** contain four-coordinate metal(II) ions, having a highly distorted tetrahedral configuration. In the case of **4** and **5**, two independent molecules exist in the asymmetric unit. For the tables and the geometric comparisons in this paper, the independent molecules in **4** and **5** are denoted as **4A**, **4B** and **5A**, **5B**, respectively. The difference

(44) Pflugrath, J. W. CrystalClear, ver. 1.3. *Acta Crystallogr.* **1999**, *D55*, 1718.
(45) Altomare, A.; Cascarano, G.; Giacovazzo, C.; Guagliardi, A.; Burla, M. C.; Polidori, G.; Camalli, M. *J. Appl. Crystallogr.* **1994**, *27*, 435.
(46) Beurskens, P. T.; Admiraal, G.; Beurskens, G.; Bosman, W. P.; de Gelder, R.; Israel, R.; Smits, J. M. M. *The DIRDIF-99 program system*; Technical Report of the Crystallography Laboratory; University of Nijmegen: Nijmegen, The Netherlands, 1999.
(47) *CrystalStructure 3.51: Crystal Structure Analysis Package*; Rigaku and Rigaku/MSC: The Woodlands, TX, 2003.
(48) *Crystal Issue 10*; Watkin, D. J.; Prout, C. K.; Carruthers, J. R.; Betteridge, P. W. Chemical Crsytallography Laboratory: Oxford, U.K., 1996.
(49) Kitajima, N.; Tamura, N.; Tanaka, M.; Moro-oka, Y. *Inorg. Chem.* **1992**, *31*, 3342.

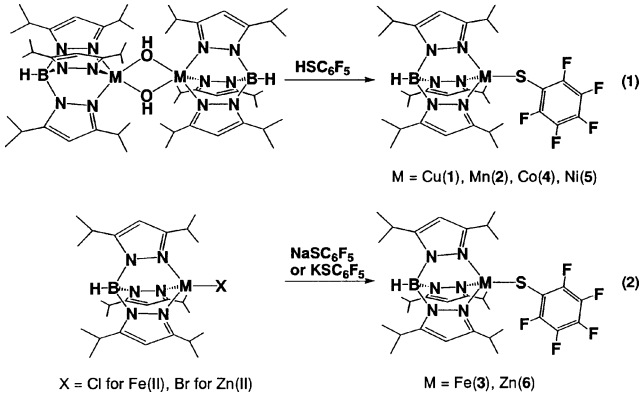

between **4A** and **4B** is the orientation of methyl groups on the next carbon of N22. In the case of **5A** and **5B**, the orientation of methyl groups on the next carbon of N21 and the orientation of each benzene ring are different. The geometries of both **4** and **5** are consistent with those of **1**−**3** and **6**. The N−M−N angles (N11−M−N21, N11−M−N31, and N21−M−N31) are about 90°, which are more acute than an ideal value of 109.7°, while the S−M−N angles (S−M−N11, S−M−N21, and S−M−N31) are ca. 100−130°, which are more obtuse than an ideal one. Thus, the ligand L attributes to the structural distortions of these complexes. This is the general tendency of other Cu(II) complexes with hydrotris(pyrazlyl)borate ligands.[50]

In comparison with the structurally characterized cobalt(II) thiolato complex [Co{HB(3,5-Me_2pz)$_3$}(SC_6F_5)], the distances of Co−S bond and all Co−N bonds are almost the same. However, this complex is slightly distorted, having the larger S−Co−N11 angle and the smaller N11−Co−N31 angle, because of the smaller ligand substitutions as compared with L.[24]

For complexes **1**−**6** the distance (*d*) between the N11N31S plane and metal(II) ion varies, depending on the structure, as shown in Figure 3. The *d* value for an ideal tetrahedral configuration is ca. 0.7 Å, and that for a general trigonal one is 0 Å. Deviations from an ideal tetrahedral configuration are evident from the plot of the *d* value vs the complex number as shown in Figure 4. The *d* value decreases from 0.43 Å in Mn(II) (**2**) to 0.28 Å in Ni(II) (**5**) and again increases to 0.41 Å in Zn(II) (**6**). The exception is Fe(II) (**3**) which has a *d* value of 0.26 Å and is thus smaller than the *d* values for either Co(II) (**4**) or Ni(II) (**5**). The reason for the deviation in this trend in **3** is not clear, as changes in the Fe(II)−N bond distances of **3** paralleled those of the other complexes (see below). These results reflect that Mn(II) and Zn(II) ions prefer a tetrahedral geometry as opposed to a highly distorted tetrahedral one, while Fe(II), Co(II), Ni(II), and Cu(II) ions can take on either geometry that is suitable for the ligands.[51]

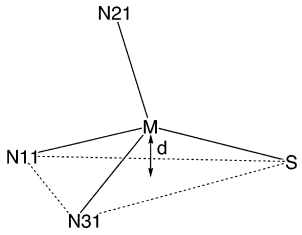

Figure 3. Model of a highly distorted tetrahedral configuration.

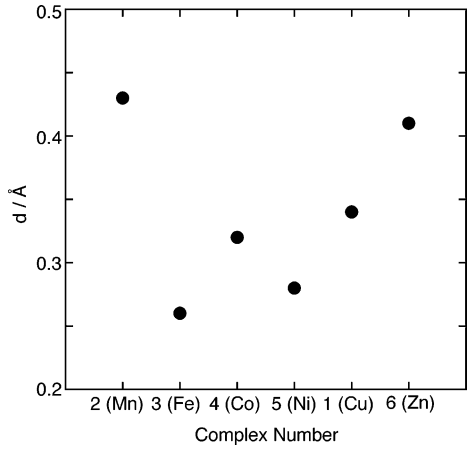

Figure 4. Plot of *d* values, which was defined as the distance between metal ion and N11N31S plane, for highly distorted tetrahedral compounds **1**−**6**.

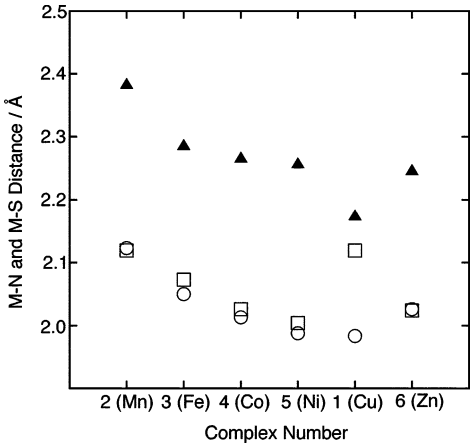

Figure 5. Plots of M−N and M−S distances for highly distorted tetrahedral compounds **1**−**6**: M−N distances which contain the N11N31S plane (○); M−N21 distance which does not contain the N11N31S plane (□); M−S distances (▲).

The values obtained by taking an average of M−N11 and M−N31 distances show a decreasing trend on going from Mn(II) (**2**) at 2.12 Å to Fe(II) (**3**) at 2.05 Å, to Co(II) (**4**) at 2.02 Å, to Ni(II) (**5**) at 1.99 Å and then an increase on going to Zn(II) (**6**) at 2.03 Å, as shown in Figure 5. The M−N21 distances in **2**−**6** also show a similar trend. The exception in **1** arises from the Jahn−Teller effect against Cu−N21 axis, resulting in the long Cu−N21 distance compared with other two Cu−N distances. In addition, the Cu−S distance in **1** is the shortest M−S bond distance in the series because of the high covalency of the Cu−S bond.[29] From these results, the *d* values and the bond angles are good indicators for these structural distortions, depending on the central metal(II) ions. Similar tendencies have been reported by Stack et al. for

(50) For recent book and reviews: (a) Parkin, G. *Chem. Commun.* **2000**, 1971. (b) Trofimenko, S. *Scorpionates-The Coordination Chemistry of Polypyrazolylborate Ligands*; Imperial College Press: London, 1999. (c) Kitajima, N.; Tolman, W. B. *Prog. Inorg. Chem.* **1995**, *43*, 419.

(51) Cotton, F. A.; Wilkinson, G.; Murillo, C. A.; Bochmann, M. *Advanced Inorganic Chemistry*, 6th ed.; John Wiley & Sons: New York, 1999.

Table 3. Absorption Spectral Data (λ/nm (ϵ/M^{-1} cm^{-1})) for Complexes **1** and **3**−**5** at Room Temperature

complex	sulfur-to-metal(II) charge-transfer bands (ϵ)	d−d bands (ϵ)
Cu (**1**)[a]	663 (5980)	1040 (1170)
Fe (**3**)[b]	308 (5940), 355 (1390)	1360 (95)
Co (**4**)[b]	311 (5030), 340 (2930)	605 (broad, 1170), 812 (140), 1479 (115)
Ni (**5**)[b]	357 (1850), 434 (3100)	804 (145), 1400 (35)

[a] Dichloromethane solution. [b] Cyclohexane solution.

the changes of M−N distances in [M(Cl)(PY5)] (PY5 = 2,6-bis(bis(2-pyridyl)methoxymethyl)pyridine; M = Mn(II), Fe(II), Co(II), Ni(II), Cu(II), and Zn(II)).[52]

The structures of blue copper proteins such as azurin,[5b] plastocyanin,[5a] pseudoazurin,[5c] amicyanin,[5d] cucumber basic protein,[5e] stellacyanin,[5f] rusticyanin,[5g] and many others have been reported. The Cu−S distance in **1** is almost the same as in those of blue copper proteins.[25] Metal(II)-substituted azurins to Ni(II), Co(II), Zn(II), and Cd(II) from Cu(II) have been reported in terms of their crystal structures,[6−9,18] UV−vis absorption,[10−11] and other spectroscopic properties.[12−15]

The M−S bond lengths of **4**−**6** are almost the same as the corresponding metal(II)-substituted azurins (Table 2). The *d* values of **4**−**6** suggest that their coordination geometries are more tetrahedrally distorted than those of native azurin or metal(II)-substituted azurins, and the bond distances from metal(II) to N21, which is in the axial position, do not show any large differences. To discuss this factor, the bond angles of **1**−**6** were compared with the corresponding metal(II)-substituted azurins. Although the S−M−N11 and N11−M−N31 bond angles in **1**−**6** are smaller than those of corresponding azurins, it is clear that the S−M−N11 and S−M−N21 bond angles are more obtuse than the N11−M−N31 bond angle. The two imidazole rings of histidines in azurins are more flexible than the tripodal N_3 ligand in **1**−**6**, and for this reason, there are some differences between the bond angles in azurins and the model complexes (see below). The *d* values of **1**−**6** are similar to that of plastocyanin, because there are no interactions of the fifth coordination atom (the opposite position to Met92) of plastocyanin.

UV−Vis Spectrscopy. The UV−vis absorption spectra of **1**−**6** were measured using cyclohexane (200−1700 nm) or dichloromethane (260−1400 nm) solution under an argon atmosphere. The assigned absorption bands are listed in Table 3. Their spectra in the region of 300−900 nm are shown in Figure 6. The low-temperature spectra using dichloromethane solution are plotted in Figure S6 (Supporting Information). The spectrum of **1** is unique and is in good agreement with that of native azurin. The assignments of the observed bands at 663 and 1040 nm in **1** were made by comparing to those of [CuL($SCPh_3$)][29] and the mononuclear copper(II) cumylperoxo complex [CuL($OOCMe_2Ph$)].[53]

The d−d transition band patterns of **3**−**5** are consistent with those of a distorted tetrahedral geometry. For **3**, one band was observed at 1360 nm, which is assigned as a d−d transition band, since the analogous complex [FeL(SC_6H_4-4-^{t}Bu)] has a similar band at ca. 1320 nm.[54] In addition, the molar extinction coefficient of **3** is consistent with a d−d transition band.[55] In general, Co(II) complexes with a pseudotetrahedral geometry have d−d transition bands in the ca. 600−2200 nm region.[55] Three bands were observed at 605, 812, and 1479 nm for complex **4**. Moreover, a shoulder band was also observed at 575 nm. The analogous complex, [Co{HB(3,5-$Me_2pz)_3$}(SC_6F_5)], shows three d−d transition bands at 570 (270), 605 (350), and 660 nm (95 M^{-1} cm^{-1}).[24] Both complexes have a band at 605 nm, but the ϵ value of **4** is much larger than that of [Co{HB(3,5-$Me_2pz)_3$}(SC_6F_5)]. In addition, there are two higher wavelength bands (812 and 1497 nm) in **4** and the corresponding bands in the spectrum of [Co{HB(3,5-$Me_2pz)_3$}(SC_6F_5)] cannot be assigned due to smaller molar extinction coefficient. Accordingly, the three bands of **4** are assigned to d−d transition bands. In general, Ni(II) complexes with a pseudotetrahedral geometry containing sulfur ligand have d−d transition bands in the ca. 800−1500 nm region.[55] In this context, the two bands at 804 and 1400 nm for **5** may be assigned to the d−d transition bands. The spectra of **2** and **6** exhibit no absorption bands above 300 nm. For **2**, the reason is that in high-spin d^5 Mn(II) complexes the d−d bands are spin forbidden as well as Laporte forbidden; thus, they are generally very weak.[55] In **6**, Zn(II) ion has a stable d^{10} electron configuration, and thus, no d−d transitions are possible.

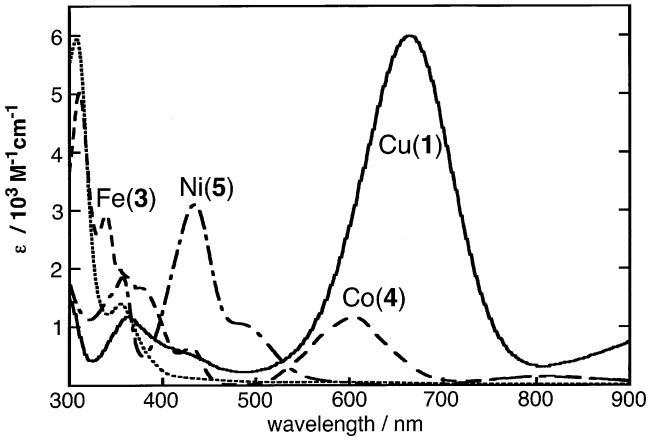

Figure 6. UV−vis absorption spectra of [ML(SC_6F_5)] (M = Cu (**1**) (—), Fe (**3**) (···), Co (**4**) (---), Ni (**5**) (— - —) at room temperature.

The one or two bands, which are assigned to the sulfur-to-metal(II) CT bands, should be observed for the spectra of **3**−**5** in the 300−500 nm region. In the case of **3**, two bands were found at 308 and 355 nm. The reported model complexes such as $(Et_4N)_2$[Fe(S_2-*o*-xyl)$_2$] (S_2-*o*-xyl = bis(*o*-xylyl-α,α′-dithiolato anion))[56] and $(Et_4N)_2$[Fe($SEt)_4$][57] have two bands, one at ∼320 nm with very strong extinction

(52) Gebbink, R. J. M. K.; Jonas, R. T.; Goldsmith, C. R.; Stack, T. D. P. *Inorg. Chem.* **2002**, *41*, 4633.
(53) Chen, P.; Fujisawa, K.; Solomon, E. I. *J. Am. Chem. Soc.* **2000**, *122*, 10177.
(54) Pavel, E. G.; Kitajima, N.; Solomon, E. I. *J. Am. Chem. Soc.* **1998**, *120*, 3949.
(55) Lever, A. B. P. *Inorganic Electronic Spectroscopy*, 2nd ed.; Elsevier Science Publishing Co., Inc.: New York, 1984.
(56) Lane, R. W.; Ibers, J. A.; Frankel, R. B.; Papaefthymiou, G. C.; Holm, R. H. *J. Am. Chem. Soc.* **1977**, *99*, 84.
(57) Hagen, K. S.; Watson, A. D.; Holm, R. H. *J. Am. Chem. Soc.* **1983**, *105*, 3905.

coefficient (7100−7750 M^{-1} cm^{-1}) and another band as a shoulder at ~350 nm. For $(Et_4N)_2[Fe(S_2\text{-}o\text{-}xyl)_2]$, both bands are assigned as CT bands.[56] The spectral behavior and band positions of **3** are very similar to those of these complexes. Thus, the assignments of both bands for **3** are the sulfur to Fe(II) CT bands. In the spectra of **4**, two bands were observed at 311 and 340 nm. The sulfur to Co(II) CT bands of $(Et_4N)_2[Co(S_2\text{-}o\text{-}xyl)_2]$[56] and $\{P(C_6H_5)_4\}_2[Co(SC_6H_5)_4]$[58] are observed at 355 (3450) and 420 nm (3000 M^{-1} cm^{-1}), respectively. Moreover, the CT band of $[Co\{HB(3,5\text{-}Me_2pz)_3\}(SC_6F_5)]$ is calculated at 289 nm.[24] Thus, the two bands in **4** are assigned to the sulfur to Co(II) CT bands. In addition, the band at the high-energy side at 311 nm is much stronger than that at the low-energy side at 340 nm, which is in good agreement with the Co(II) derivative of azurin,[10] in which both bands at 330 (3020) and 375 nm (1180 M^{-1} cm^{-1}) are assigned to the sulfur to Co(II) CT bands.[10b] For **5**, two bands were observed at 357 and 434 nm. The band of $(Et_4N)_2[Ni_2(S_2\text{-}o\text{-}xyl)_3]$ is observed at 486 nm (3760 M^{-1} cm^{-1}), which is assigned to sulfur to Ni(II) CT bands.[56] Moreover, Ni(II)-substituted azurin has two bands at 358 (3098) and 440 nm (3060 M^{-1} cm^{-1}),[10b] which are very similar with those of **5**. Therefore, both bands are assigned to the sulfur to Ni(II) CT band. These results confirm that the complexes **4** and **5** are good structural models for metal(II)-substituted blue copper proteins and the relationship of the metal to the N_2S basal plane is a very important factor in determining d−d transition energies and sulfur-to-metal(II) CT energies. Moreover, the CT energies of Fe(II) (**3**), Co(II) (**4**), and Ni(II) (**5**) are each shifted to higher energy relative to that of **1**.

Magnetic and Electrochemical Properties. Magnetic susceptibility was discussed only for **4** and **5** because they are not oxygen and/or temperature sensitive.[59] The Co(II) complex **4** exhibits an effective magnetic moment $\mu_{eff} = 4.62$ μ_B at 296 K. In general, the magnetic moments of high-spin tetrahedral Co(II) complexes are in the range from 4.6 to 4.8 μ_B.[51] Therefore, this supports a high-spin configuration for **4**. For the Ni(II) complex **5**, $\mu_{eff} = 3.30$ μ_B was obtained at 293 K. This value is similar to the reported effective magnetic moment of Ni(II)-substituted azurin, 3.2 μ_B by Balzack et al.[14g] and 2.8 μ_B by Jiménez et al.[15] In contrast, the magnetic moment of tetrahedral Ni(II) complexes including distortions varies from 3.00 to 4.0 μ_B.[51] Therefore, this result shows good agreement with those of the Ni(II)-substituted azurin.

While EPR spectra of all complexes were measured, only **1**, **2**, and **4** showed EPR signals (Figure S7). No signal is anticipated for **3** or **5**, as these are high-spin distorted tetrahedral Fe(II) and Ni(II) complexes with integer spins of $S = 2$ and $S = 1$, respectively. While EPR signals were observed for **1** and **2** at both 140 and 20 K, the signals of **4** only appeared below 20 K. The EPR spectrum of **1** is axial with $g_{\|} = 2.32$, $g_{\perp} = 2.10$, and $A_{\|} = 52$ G.[25] These EPR parameters are very similar to those of native azurin[5b] and plastocyanin[5a] and reflecting the *d* values as described above.

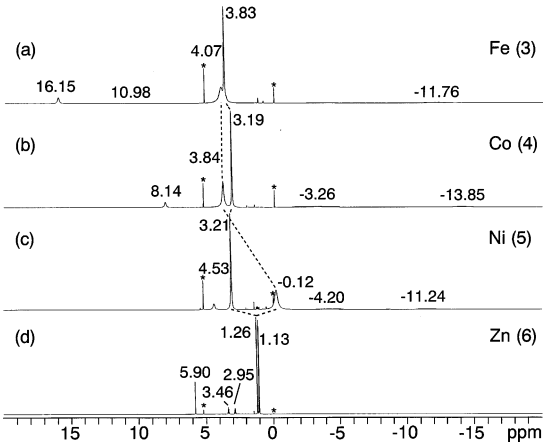

Figure 7. ^1H NMR spectra of $[ML(SC_6F_5)]$ (M = Fe (**3**) (a), Co (**4**) (b), Ni (**5**) (c), Zn (**6**) (d)) at room temperature (expansion from 20 to −20 ppm).

For **2**, the EPR spectrum shows a signal of $g = 3.91$. The spectral pattern of **2** is similar to that of Mn(II) superoxide dismutase[60] or Mn(II) catechol dioxygenase.[61] Unfortunately, the EPR signals of the Mn(II)-substituted blue copper proteins have not been published.[10d] However, this report has been made that indicates the Mn(II) ion is spontaneously released from Mn(II)-substituted azurin.[10d] This result indicates that the active sites of the native blue copper proteins have a semirigid ligand environments compared with the N_3 tripodal ligand. The spectral behavior of **4** ($g_1 = 5.90$, $g_2 = 2.66$, and $g_3 = 1.74$) is similar with that of Co(II)-substituted azurin.[6,10d] In addition, the temperature dependence and spectral pattern indicate **4** is high spin.[10d]

The paramagnetic ^1H NMR spectra were measured for the Fe(II), Co(II), and Ni(II) complexes (**3**−**5**). These results are shown in Figure 7 (expansion from 20 to −20 ppm) and Figure S8 (all region) with the spectrum of the Zn(II) complex **6**. The previous assignments of Fe(II) complexes are used.[43,62−63] In general, the protons near to the metal(II) ions suffer the largest chemical shift and the greatest line broadening. However, the 4-H protons of the pyrazolyl ring were observed to have the largest downfield shift in 65−80 ppm region, having an integration of 3 protons (Figure S8). This is a general tendency for complexes containing the hydrotris(pyrazolyl)borate ligand.[43,62−63] The large shift comes from the deshielding effects of the aromatic pyrazolyl ring current.[64] The signals are gradually shifted downfield, going from 66.11 ppm for **3**, to 73.67 ppm for **4**, and to 81.09 ppm for **5**. Furthermore, the methyl protons of its isopropyl group are observed in the narrow region from −2

(58) Swenson, D.; Baenziger, N. C.; Coucouvanis, D. *J. Am. Chem. Soc.* **1978**, *100*, 1932.
(59) The fatal color changes of **1**−**3** were observed during grinding.
(60) Whittaker, J. W.; Whittaker, M. M. *J. Am. Chem. Soc.* **1991**, *113*, 5528.
(61) Whiting, A. K.; Boldt, Y. R.; Hendrich, M. P.; Wackett, L. P.; Que, L., Jr. *Biochemistry* **1996**, *35*, 160.
(62) Kitajima, N.; Tamura, N.; Amagai, H.; Fukui, H.; Moro-oka, Y.; Mizutani, Y.; Kitagawa, T.; Mathur, R.; Heerwegh, K.; Reed, C. A.; Randall, C. R.; Que, L., Jr.; Tatsumi, K. *J. Am. Chem. Soc.* **1994**, *116*, 9071.
(63) Mehn, M. P.; Fujisawa, K.; Hegg, E. L.; Que, L., Jr. *J. Am. Chem. Soc.* **2003**, *125*, 7828.
(64) Ming, L.-J. In *Physical Methods in Bioinorganic Chemistry: Spectroscopy and Magnetism*; Que, L., Jr., Ed.; University Science Book: Sausalito, CA, 2000.

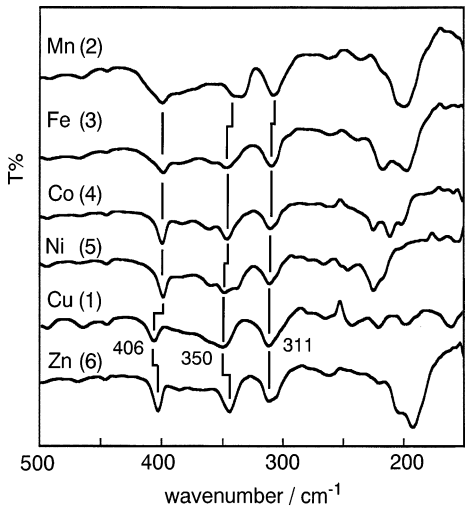

Figure 8. Far-IR spectra of **1**−**6**.

to 5 ppm. The methyl protons near the boron atom are almost not shifted, Fe(II) 3.83, Co(II) 3.19, and Ni(II) 3.21 ppm. However, the other methyl protons near the metal(II) ion are broadened and shifted without order of the d electron numbers, Fe(II) 4.07, Co(II) 3.84, and Ni(II) −0.12 ppm. Other broad signals of the methine protons of its isopropyl group and B−H proton are also shifted without order.

There have been many reports concerning the paramagnetic ^{1}H NMR spectra of Co(II)- and Ni(II)-substituted azurin. However, the maximum chemical shifts in the spectra of both metal substituted azurins are found at much lower magnetic field than those of **4** and **5**. Larger shifts and broader line widths are observed compared in the spectra of Co(II)-substituted azurin as compared to Ni(II)-substituted azurin.[5b,10a,14a,14d,14h] Moreover, the protons of His46 and His117 are in the −10 to 100 ppm region for Co(II)-substituted azurin and the −15 to 65 ppm region for Ni(II)-substituted azurin. However, the protons of Cys112 show the largest chemical shift (ca. 240 ppm) in both spectra. The chemical shifts of the protons on pyrazolyl rings (**4** and **5**) fall into the same region with those on imidazole rings.

Cyclic voltammetric examinations of **2**−**6** in acetone under argon were carried out. However, they showed no clear peaks. Only **1** in the same condition shows a single reversible redox signal at −468 mV versus Fc^+/Fc as shown in Figure S9. On the basis of this reversibility, it corresponds to Cu(II)/Cu(I) process. The redox signal of [CuL(SMeIm)] (HSMeIm = 2-mercapto-1-methylimidazole) was clearly shifted to −912 mV versus Fc^+/Fc.[34,65] This means that **1** is very easily reduced to Cu(I) state rather than [CuL(SMeIm)].

M−S Stretching Vibration. The far-IR spectra of complexes **1**−**6** are shown in Figure 8. All three far-IR bands in **1** at 406, 350, and 311 cm^{-1} are assigned to Cu−S stretching vibration from resonance Raman results of **1**[28] and native azurin.[66] The spectra in **2**−**6** show almost the same behavior as **1** in the 300−500 cm^{-1} region. However, all bands are slightly shifted from **1** in this region, depending on their structures.

The largest shifts were observed for bands at ca. 400 cm^{-1} (403 ± 4 cm^{-1}), which has the most M−S stretching character.[28] It reflects the changes in M−S bond distances, from 2.176(4) Å in **1** to 2.248(2)−2.385(3) Å in **2**−**6**, reflecting the higher covalency of the Cu−S bond as compared to the other metal(II)-substituted complexes. Similar shifts are observed in the resonance Raman spectra of native and Ni(II)-substituted azurin.[11] Complexes **1**−**6** all have the same bands at ca. 310 cm^{-1} (from 308 to 311 cm^{-1}). However, the bands at ca. 350 cm^{-1} may be divided into two groups, **2** and **6** (average, 341 cm^{-1}) and **3**−**5** (average, 347 cm^{-1}). These differences arise from the central metal(II) geometries. Complexes **2** and **6** have larger *d* values (average, 0.42 Å), whereas complexes **3**−**5** have smaller *d* values (average, 0.29 Å). These two bands are therefore very sensitive to the coordination geometry.

As mentioned before, the Raman shifts in **1**[28] are consistent with the far-IR spectra of **1**. Therefore, the far-IR spectra are good indicators for all metal(II)-substituted model complexes (**1**−**6**).[67] Moreover, we observed the Raman shifts of **2** and **6**: Mn (**2**), 385, 332, and 308 cm^{-1}; Zn (**6**), 401, 339, and 311 cm^{-1} (Figure S10). Therefore, we can obtain fundamental information about the M−S stretching vibration by comparing far-IR spectra (**1**−**6**) and FT-Raman spectra (**2** and **6**). The detailed assignment will be performed for **4** and **5** by resonance Raman spectroscopy.

Summary and Biological Relevance The metal-substituted complexes [ML(SC_6F_5)] were synthesized using Mn(II) (**2**), Fe(II) (**3**), Co(II) (**4**), Ni(II) (**5**), and Zn(II) (**6**) as models for metal(II)-substituted azurins. All the complexes were characterized by UV−vis absorption and far-IR spectroscopies and other properties. Moreover, the complexes of **4** and **5** were compared with metal(II)-substituted azurins. All complexes have a highly distorted tetrahedral geometry, which is the same as the corresponding metal(II)-substituted azurins. In the UV−vis absorption spectra, the d−d bands of **3**−**5** are assigned and have the same energy as distorted tetrahedral geometry. Moreover, the sulfur-to-metal(II) CT bands are shifted to higher energy in **3**−**5** rather than in **1**. Their M−S stretching vibration energies and other physicochemical properties are consistent with their structural distortions. The properties of metal(II)-substituted azurins are very similar to those of model complexes of **4** and **5**. Therefore, the relationship of the metal(II) to the N_2S basal plane is a very important factor for these properties as indicated in **1**. We can summarize the structural and spectroscopic behavior upon increasing the number of d electrons as follow: (1) Distance *d* is consistent with the

(65) Basumallick, L.; DeBeer George, S.; Randall, D. W.; Hedman, B.; Hodgson, K. O.; Fujisawa, K.; Solomon, E. I. *Inorg. Chim. Acta* **2002**, *337*, 357.

(66) Andrew, C. R.; Han, J.; den Blaauwen, T.; van Pouderoyen, G.; Vijgenboom, E.; Canters, G. W.; Loehr, T. M.; Sanders-Loehr, J. *J. Biol. Inorg. Chem.* **1997**, *2*, 98.

(67) Since the complexes with Mn(II) (**2**), Fe(II) (**3**), and Zn(II) (**6**) have no color, we cannot collect any M−S stretching frequencies by resonance Raman spectroscopy.

ionic radius and the general coordination preference of each metal(II) ion except for **3** (Figure 4). (2) From UV−vis absorption spectra of **1**, **4**, and **5**, the sulfur-to-metal(II) CT bands are shifted to higher energy (Figure 6). (3) The downfield-shifted proton signals of the pyrazolyl 4th position in ^{1}H NMR spectrum of **3**−**5** are observed with order (Figure S8). Moreover, the electron configurations around the metal(II) ions of **4** and **5** are suggested to be similar to those of the corresponding metal(II)-substituted azurin from ^{1}H NMR and EPR spectra (Figures 7 and S7). Only **1** shows a single reversible redox signal in cyclic voltammograms (Figure S9). This indicates that the copper(II) ion is most suitable for electron-transfer reactions in this distorted tetrahedral geometry, so that in nature the proteins select this Cu(II) ion for fast electron-transfer reaction. However, we need more detailed experiments for their assignments and roles of metal(II) ions in the electron-transfer reaction mechanism including the relationship between structure and function of electron transfer.

Acknowledgment. This research was supported in part by the Japan Society of the Promotion of Science (Grant Nos. 13555257 and 14350471) and by the Ministry of Education, Culture, Sports, Science, and Technology (the 21st Century COE program (Promotion of Creative Interdisciplinary Materials Science for Novel Function)). Finally, we appreciate the kind editing of this manuscript by Dr. Serena DeBeer George of the Stanford Synchrotron Radiation Laboratory.

Supporting Information Available: Complete listings of atomic coordinates for **2**−**6** (Figures S1−S5), temperature factors, bond lengths, bond angles, and torsion angles for all structures **2**−**6** (Tables S1−S5), UV−vis absorption spectra of **1** and **3**−**5** at −45 °C (Figure S6), EPR spectra of **1**, **2**, and **4** (Figure S7), ^{1}H NMR spectra of **3**−**6** (all regions) (Figure S8), cyclic votammograms of **1** (Figure S9), FT-Raman spectra of **3** and **6** (Figure S10), and crystallographic data in CIF format. This material is available free of charge via the Internet at http://pubs.acs.org.

IC049814X